

See discussions, stats, and author profiles for this publication at: <https://www.researchgate.net/publication/234927320>

Energy deposition model for low-energy electrons (10–10 000 eV) in air

Article in *Journal of Applied Physics* · May 2004

DOI: 10.1063/1.1704864

CITATIONS

28

READS

1,062

5 authors, including:



Antonio Muñoz Roldan

Centro Investigaciones Energéticas, Medioambientales y Tecnológicas

71 PUBLICATIONS 1,235 CITATIONS

[SEE PROFILE](#)



Jose M Pérez

Centro Investigaciones Energéticas, Medioambientales y Tecnológicas

104 PUBLICATIONS 2,603 CITATIONS

[SEE PROFILE](#)



Gustavo Garcia

Spanish National Research Council

381 PUBLICATIONS 6,471 CITATIONS

[SEE PROFILE](#)

Some of the authors of this publication are also working on these related projects:



positrons in gases and liquids, positrons in medicine [View project](#)



positron gas filled traps [View project](#)

Energy deposition model for low-energy electrons (10–10 000 eV) in air

A. Roldán and J. M. Pérez

Centro de Investigaciones Energéticas Medioambientales y Tecnológicas, Avenida Complutense 22, 28040 Madrid, Spain

A. Willart

Departamento de Física de los Materiales, Universidad Nacional de Educación a Distancia, Senda del Rey 9, 28040 Madrid, Spain

F. Blanco

Departamento de Física Atómica, Molecular y Nuclear, Universidad Complutense de Madrid, Avenida Complutense s.n., 28040 Madrid, Spain

G. García^{a)}

Instituto de Matemáticas y Física Fundamental, Consejo Superior de Investigaciones Científicas, Serrano 121, 28006 Madrid, Spain

(Received 9 September 2003; accepted 23 February 2004)

An energy deposition model for electrons in air that can be useful in microdosimetric applications is presented in this study. The model is based on a Monte Carlo simulation of the single electron scattering processes that can take place with the molecular constituents of the air in the energy range 10–10 000 eV. The input parameters for this procedure have been the electron scattering cross sections, both differential and integral. These parameters were calculated using a model potential method which describes the electron scattering with the molecular constituent of air. The reliability of the calculated integral cross section values has been evaluated by comparison with direct total electron scattering cross-section measurements performed by us in a transmission beam experiment. Experimental energy loss spectra for electrons in air have been used as probability distribution functions to define the electron energy loss in single collision events. The resulting model has been applied to simulate the electron transport through a gas cell containing air at different pressures and the results have been compared with those observed in the experiments. Finally, as an example of its applicability to dosimetric issues, the energy deposition of 10 000 eV by means of successive collisions in a free air chamber has been simulated. © 2004 American Institute of Physics. [DOI: 10.1063/1.1704864]

I. INTRODUCTION

Important radiological and dosimetric applications require detailed energy deposition models of electrons interacting with matter, not only in terms of the total absorbed dose but giving the energy distribution along the particle tracks. Energetic particles (photon, electron or ion) passing through matter produce secondary electrons that are mainly responsible for the energy transfer by means of successive collisions with the constituent atoms or molecules. Therefore these models should consider secondary electron interactions, at molecular level, over a wide energy range. In principle, energies from the incident particle energy down to the final step of the energy degradation procedure should be considered. However, the great diversity of possible processes in this range makes difficult a complete treatment of the problem, being necessary reasonable approximations supported by experiments. Among the wide variety of targets of interest in these applications, air is one of the most suitable, as long as this gas is commonly adopted as a reference radiological

material and usually fills the ionization chambers which are the basis of some radiation detectors. Monte Carlo methods are commonly used to simulate the electron interaction and transport through the matter. Most of them use, as input parameters, cross section data calculated in the framework of the first Born approximation.¹ However, we have shown in previous studies^{2,3} that, for energies below 10 000 eV, this approximation overestimates the total electron scattering cross sections from several molecular targets, as those constituting air, reaching discrepancies of the order of 40% for energies below 1000 eV. Therefore models based on a more precise description of the electron scattering processes are needed at these energies.

These considerations motivated this work. The aim of this study is to obtain a realistic energy deposition model for electrons in air, based on a Monte Carlo simulation of the particle tracks and the energy losses derived from single electron scattering events with the main molecular constituent of air, namely N₂ and O₂. The simulation program was based on the Geant4⁴ code with significant modifications demanded by the physics of this problem. The main input parameters are the electron interaction cross sections, both differential and integral, corresponding to the most probable processes occurring in the considered energy range (10–

^{a)} Author to whom correspondence should be addressed. Instituto de Matemáticas y Física Fundamental, Consejo Superior de Investigaciones Científicas, Serrano 121, 28006 Madrid, Spain; electronic mail: g.garcia@imaff.cfmac.csic.es

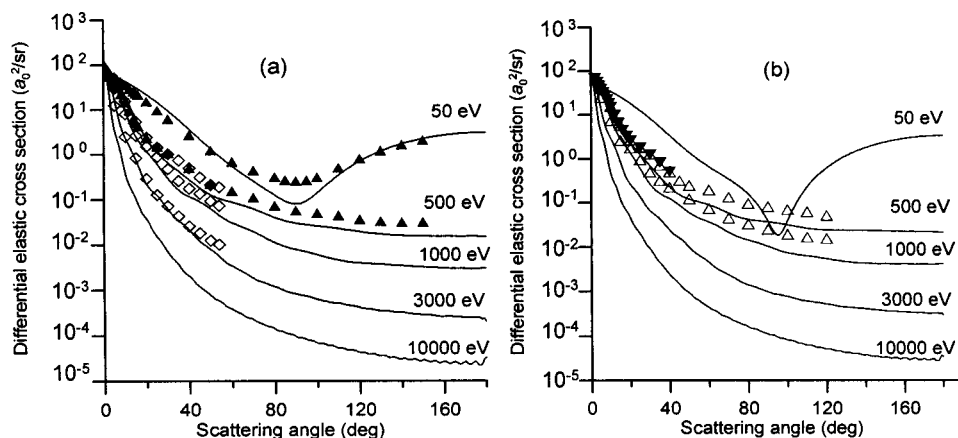


FIG. 1. Differential elastic cross sections for electron scattering from (a) N_2 , (b) O_2 . —, present calculation; \blacktriangle , DuBois and Rudd (see Ref. 12); \diamond , Jansen *et al.* (see Ref. 13); \blacktriangledown , Bromberg (see Ref. 14); \triangle , Iga *et al.* (see Ref. 15).

10 000 eV). The required electron scattering cross-sections data have been calculated for N_2 and O_2 by using an improved optical potential procedure.⁵ The air composition assumed for these calculations, as well as the reliability of the calculation procedure have been checked by comparison with accurate measurements (within 3%) of the total electron scattering cross sections from air performed in a transmission beam experiment. Normalized energy loss distribution functions have been derived from the experimental energy loss spectra obtained with the same experimental system.

The present energy deposition model has been applied to simulate the electron beam transport through a gas cell containing air at different pressures. The energy and intensity distributions of the simulated transmitted beam will be discussed by comparison with the experimental results. Finally, the applicability of this energy deposition model to dosimetric issues has been shown by simulating the particle tracks and the energy degradation process of 10 000 eV electrons passing through a chamber filled with air at atmospheric pressure.

II. CROSS SECTION DETERMINATION PROCEDURE AND ENERGY LOSS SPECTRA

A. Differential and integral electron scattering cross section calculations

The principles of the optical potential procedure followed to calculate differential and integral electron scattering cross sections from molecules have been described in previous papers.^{6,7} Basically, we have considered that the incident electron energy is appropriate for the application of the independent atom model.⁸ The electron–atom interaction is then represented by an approximate optical potential given by

$$V_{\text{opt}}(r) = V(r) + iV^a(r) \\ = V_s(r) + V_e(r) + V_p(r) + iV^a(r), \quad (1)$$

where the real part $V(r)$ is the effective atomic potential which includes three terms: the static potential calculated from the charge density derived from a relativistic Hartree–Fock procedure⁹ $V_s(r)$, the exchange potential $V_e(r)$ as defined by Riley and Truhlar¹⁰ and the polarization potential $V_p(r)$ in the form given by Zhan *et al.*¹¹ The imaginary part

$V^a(r)$ is the absorption potential derived from an *ab initio* procedure based on the *quasifree* electron model,^{6,7} including all the improvements that we have proposed recently.⁵ Following the method described in Ref. 5, the complex partial wave phase shifts derived from the above potential allowed to determine the differential elastic cross section $d\sigma_{\text{el}}(E)/d\Omega$ and, applying the optical theorem,⁸ the total absorption or integral inelastic cross sections $\sigma_{\text{inel}}(E)$. The integral elastic cross sections $\sigma_{\text{el}}(E)$ were determined by integrating the corresponding differential values for a given energy. Finally, molecular cross section data have been derived from those of the constituent atoms following the addition procedure described in Ref. 5.

The calculated differential elastic cross sections for electron scattering from N_2 and O_2 are shown in Fig. 1 for some incident energies (50, 500, 1000, 3000, and 10 000 eV), together with representative experimental data.^{12–15} Taking into account that experimental differential cross section values usually have large error limits (above 20%) because of the normalization procedures needed to obtain absolute values, there is a reasonable agreement between theory and experiment for both molecules.

Integral cross-section values for electron interaction in dry air have been determined from its molecular constituents by assuming a target composition of 78.09% N_2 and 21.19% O_2 . Results for the integral elastic, integral inelastic, and total electron scattering cross section from air are shown in Fig. 2 for energies ranging from 10 to 10 000 eV.

As will be described in the next section, the consistency of these results has been checked by comparison with direct measurements of the electron beam attenuation in air for selected energies.

B. Total electron scattering cross section and energy loss measurements

Total electron scattering cross section from air have been directly measured in the energy range 1000–5000 eV by using a transmission beam technique.¹⁶ The experimental setup is shown in Fig. 3. Both the system and the experimental procedure have been described elsewhere^{17,18} and will only be briefly reported here. The primary electron beam, produced by an emitting filament, was collimated into a 1 mm diameter beam and deflected by a combination of electro-

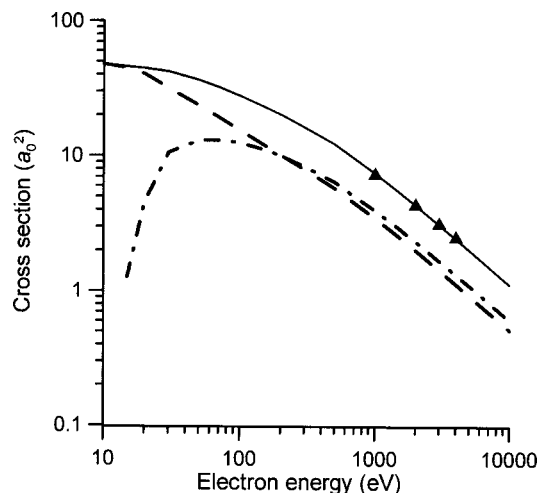


FIG. 2. Integral electron scattering cross sections from air. Present calculations:—, total electron scattering cross section;---, integral elastic cross sections;— · —, integral inelastic cross sections. Present measurements: ▲, total electron scattering cross sections.

static plates and a transverse magnetic field. Typical operating currents were between 10^{-13} to 10^{-14} A with an energy resolution of 500 meV. The collision chamber was defined by two apertures each of 1 mm diameter separated by a length of 100 mm. Electrons emerging from the collision chamber were deflected by an electrostatic plates system to select the angle of analysis. The transmitted electrons were energy analyzed by an electrostatic hemispherical spectrometer combined with a retarding field. Under these conditions a constant energy resolution of about 0.8 eV was obtained over the whole energy range considered here. The acceptance angle of the analyzer was in the order of 10^{-5} sr. Electrons were detected at the exit of the energy analyzer by a two stage microchannel plate (MCP) electron multiplier operating in pulse counting mode. The gas pressure in the chamber was measured within 1% by an absolute capacitance manometer (MKS Baratron 127 A). The ultimate pressure in the region of the energy analyzer and electron detector was lower than 10^{-6} Torr. The total cross sections were derived from the attenuation of the transmitted electron beam when the target pressure was varied from 1 to 20 mTorr. In these conditions, we have shown² that multiscattering processes are negligible and that the error contribution to the attenuation measure-

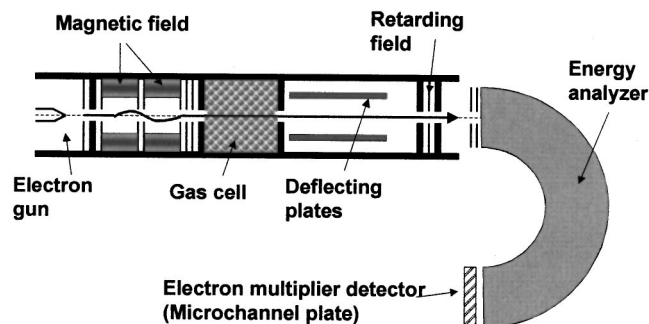


FIG. 3. Experimental setup used for total electron scattering cross sections and energy loss measurements.

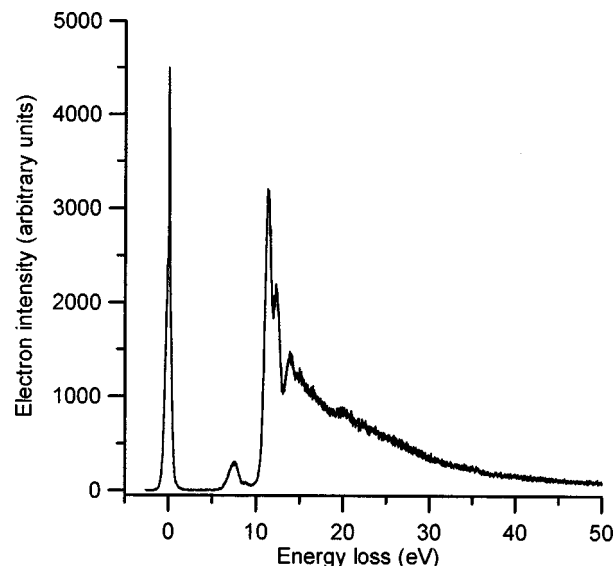


FIG. 4. Experimental energy loss spectrum at 5° for 2000 eV incident electrons and 20 mTorr of air in the collision chamber.

ments due to forward scattered electrons is less than 1%. As a combination of the partial error sources, a total experimental error of 3% can be assumed for the present total cross-section measurements.¹⁶ Experimental results for total electron scattering cross sections in air are shown in Fig. 2 together with those calculated with the above procedure. As this figure shows, for energies above 1000 eV there is a general agreement, within 5%, between the present theoretical and experimental data. We can expect a similar behavior at lower energies while the above method to calculate electron scattering from molecules is applicable, above 50 eV. Therefore, for the computing procedure proposed in this paper, the calculated integral cross-section data will be used by assuming, for this energy range, an error limit of about 7%. Below 50 eV the results of this study should be considered only qualitatively.

The electron energy loss spectra have been obtained with the same experimental system by sweeping the retarding field at the entrance of the energy analyzer with a voltage ramp generator synchronized with a multichannel system controlled by a computer. In this case, some changes in the scattering geometry have been introduced to improve the angular definition. The scattering chamber length was reduced to 10 mm while the exit aperture diameter was enlarged to 2 mm. The angle of analysis was selected by deflecting the transmitted beam with the electrostatic parallel plate system, covering an angular range from 0 to 15 degrees. For the energies considered in this experiment the differential electron scattering cross sections are strongly peaked on the forward direction, being the ratio between the intensity of electrons scattered at higher angles than 15° and that of the forward scattered electrons less than 0.1 for energies above 500 eV. A typical energy loss spectrum of electrons scattered at 5° for 2000 eV incident energy and 20 mTorr of air in the collision chamber is shown in Fig. 4. Energy spectra were recorded at different incident energies ranging from and different scattering angles between 0° and 15° . We found that

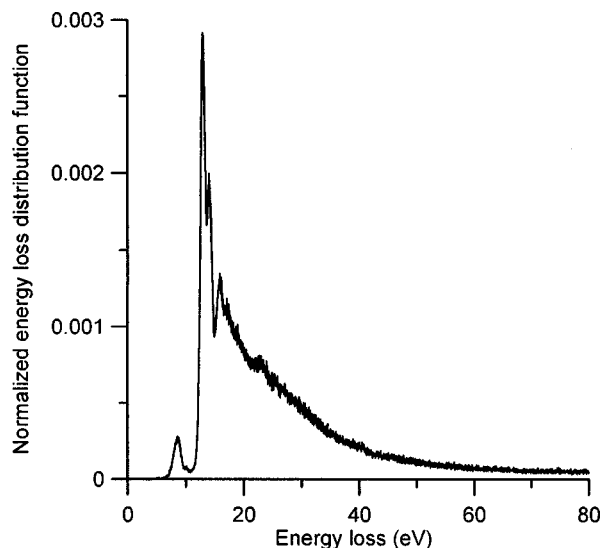


FIG. 5. Energy loss distribution function, from 0 to 80 eV, used to sample the energy deposition of inelastic collisions.

the scattered signal decreased as the scattering angle increased, but maintained the relative intensity distribution of the inelastic peaks fairly constant, within 15%, for energies above 1000 eV. We have therefore assumed a common energy loss spectrum for the whole energy range considered here. This is a rough estimation which gives the main contribution to the uncertainty quoted to this simulation procedure. The averaged experimental energy loss spectrum defined a common probability distribution function for all energies considered which was introduced in the simulation to decide the energy lost by the electrons when inelastic collisions take place. This energy loss distribution function (from 0 to 80 eV) is shown in Fig. 5.

III. MONTE CARLO SIMULATION

A. Simulation model

In order to implement a Monte Carlo simulation based on original cross-section data, two possibilities can be considered: (a) generating a totally new simulation code and (b) modifying an existing code, replacing some theoretical approximations used to describe electron interactions by input databases derived from experimental cross-section results. Since a Monte Carlo simulation involves many aspects, apart from the physics of interactions, we have concluded that the most efficient way to implement an energy deposition model at molecular level is by using reliable existing codes but introducing the degree of detail required by the mentioned applications. Thus, some advantages of significant aspects such as generation of primaries, geometry, visualization, tracking, etc., can be taken from them.

In principle, any of the highly developed codes available on the market could be used for our purpose. However, one of the largest developed codes for radiation-matter interaction simulation is Geant4.⁴ More than a single code, it is a full kit of simulation tools, the result of a vast work of more than 100 scientists and engineers from research laboratories worldwide. As an object-oriented program, the implementa-

tion of the physics to be used is open. Specifically, the Geant4 code gives the opportunity of using databases and processes different to the implemented ones, allowing new physics be tailored to the standard procedures to simulate particles and materials. Thus, the Geant4 code can naturally be used for our purposes of implementing new electron interaction models, taking advantage of its already tested tools for geometry modeling, material and particle definitions, Monte Carlo tracking of events, collection of data about interaction positions and deposited charge in sensitive materials, etc. In other words, we simply implement new physical processes in a fully operative simulation platform, in order to include low energy (below 10 000 eV) electron interaction processes according to our calculated and experimental results.

The electron elastic and inelastic interaction processes have been introduced in the code as a new program. Both, experimental and calculated cross-section data are used by this program as input parameters. Standard Monte Carlo techniques applied to the distribution functions generated from the input data decide the trajectories and energy deposition patterns of electrons in the target chamber.

Once these programs are included, electrons in the code are linked only to these effects. The standard processes in Geant4 for electrons are not considered. Thus, the physics applicable when an electron is tracked relies only on the two new processes.

The mean free path of electrons in the chamber is defined by the total electron scattering cross sections. When a single collision takes place, the program decides whether it is elastic or inelastic by pondering the related cross-section data. In a single elastic collision no energy loss of the electron is considered, but there is a change of direction given by the angular probability derived from the differential elastic cross sections computed as described above. In order to decide the angle of the emerging electron elastically scattered, the energy range considered in this study has been divided into nine bins (0–150, 150–300, 300–500, 500–700, 700–900, 900–1500, 1500–2500, 2500–3500, and 3500–10 000 eV) each one being represented by a fixed energy value: 100, 200, 400, 600, 800, 1000, 2000, 3000, and 5000 eV, respectively. The differential elastic cross sections corresponding to these representative energies have been used to derive the normalized distribution functions that have been used to sample the scattering angles. The same procedure has been carried out to decide the scattering angle when the collision was inelastic.

In the case of inelastic scattering, some amount of energy is deposited in the medium. This energy lost by the incoming electron is sorted from data tables included in the inelastic scattering class obtained from the experimental energy loss spectra. In this way, the code provides an energy loss profile and angular deflections fully compatible with our experimental results. So, in contrast with other models available in the literature, the molecular structure of the target is defining here the energy deposition pattern. In this case, the energy assigned to the scattered electron corresponds to the electron incoming energy (immediately before the interaction) minus the energy loss.

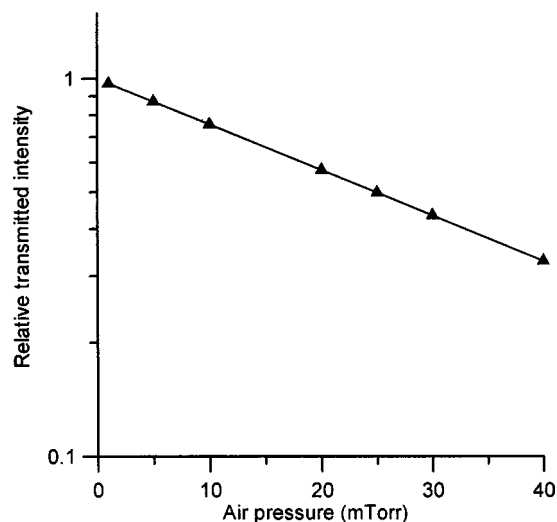


FIG. 6. Transmitted electron intensity relative to the incident electron intensity as a function of the air pressure in the gas cell for 2000 eV electrons.

The energy lost by electrons along their tracks within the gas collision chamber is stored in the code at the corresponding position. As expected, the simulated energy loss spectrum for a 2000 eV electron beam hitting the gas cell containing air at 20 mTorr is nearly coincident with the energy loss distribution shown in Fig. 5, for a significant number of histories, giving the same (within 0.1%) averaged energy loss per inelastic event, namely 33.93 eV.

B. Applications to energy deposition models

The code has first been applied to the study of the attenuation of an electron beam through the gas cell at different pressures between 2 and 40 mTorr. Two collimation apertures along the axis beam, 1 mm diameter each, placed at the entrance and exit of the chamber have been assumed to reproduce the experimental conditions. The relative intensity of the simulated transmitted beam is plotted in Fig. 6 as a function of the pressure in the chamber for 2000 eV incident electron energy. As this figure shows, the transmitted intensity follows an exponential decrease versus pressure which allows us to determine the total cross-section value for this energy. The agreement found between the experimental total cross section at this energy and that derived from the simulation (4.49 and $4.29 a_0^2$, respectively) gives an idea of the self-consistency of the simulation program developed here.

As an example of the applicability of this procedure to dosimetric issues, we have simulated particle tracks and energy deposition of 10 000 eV electrons interacting in a gas chamber with air at atmospheric pressure. Electrons interact in the gas until all its energy is deposited in it. In spite of the relatively high energy of the primary electrons, the model reproduces the experimental evidence that each electron deposits its energy through many interactions giving the already mentioned average energy loss. A viewgraph of a representative computed energy deposition map is shown in Fig. 7. As can be seen in this figure, the energy deposition model proposed in this work can be a useful complement for radiation detectors, giving additional information on how and

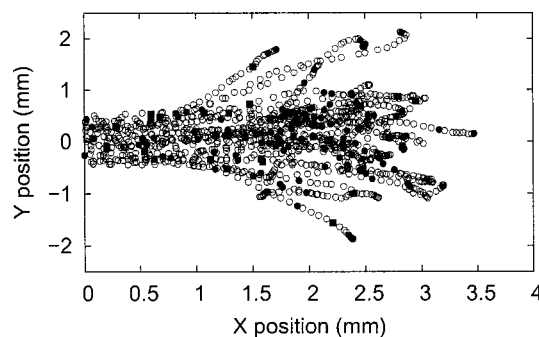


FIG. 7. Energy deposition model for 1 mm diameter electron beam of 10 000 eV entering along the X axis of a gas cell containing 1 atmosphere of air. Giving thought to the cross-section data and the energy loss spectra, the simulation procedure decides the type of single scattering event that takes place, as well as the amount of energy transferred to the medium in this process. This energy is represented by the plotted points as follows: ●, between 0 and 50 eV; ○, between 50 and 100 eV; □, higher than 100 eV. In order to clarify the graph, only one of each 10 points are plotted.

where the energy of electrons, which are generated in these detectors as secondary particles, is deposited inside the chamber. In order to assign a dose magnitude to the collected charge in these detectors some approximations are customary used, namely the assumption of local charge equilibrium at the collecting region and the use of a mean energy required to produce an electron ion pair. The present simulation procedure can also be very useful to check the reliability of these approximations for a given detector configuration, as long as precise information about interaction positions and energy deposition is available.

IV. CONCLUSIONS

In this paper we propose a detailed energy deposition model for low energy electrons in gases. The model is based on a Monte Carlo simulation which uses our experimental and theoretical electron scattering cross-section data as input parameters, as well as the observed energy loss spectra. Therefore, the developed program allows input parameters based on experimental and theoretical electron scattering data giving information on the energy distribution along the particle tracks. Since electrons are produced as secondary particles in most gaseous radiation detectors, preliminary applications to the energy deposition of electrons in air at atmospheric pressure have been also presented. Some restrictive approximations, such as the assumption of an electronic equilibrium and the definition of an average energy to produce an ion pair, are generally implicit to assess the absorbed dose in gaseous radiation detectors which are based on charge collection. Since these simplifications tend to fail when the energy decreases, their reliability can be checked through this model.

In this paper we have shown the first stage of the work in which the main features of the method have been developed, but considerable experimental effort to include more processes and to reduce the energy steps, and therefore the energy resolution, should be made to extend the applicability of this model to other radiological problems (microdosimetry, radiation damage). In order to reduce the uncertainties re-

lated to the energy loss spectra, different energy distribution functions for each energy and each scattering angle should be also considered. These aims will be the center of attention for further experiments.

ACKNOWLEDGMENTS

This work has been partially supported by the Spanish Programa Nacional de Promoción General del Conocimiento (Project No. BMF 2000-0012) and by the research program of the Universidad Nacional de Educación a Distancia (Projects Nos. 2001v/proyt/04 and 20011/ininv/37).

¹M. Inokuti, *Rev. Mod. Phys.* **43**, 297 (1971).

²G. García, M. Roteta, and F. Manero, *Chem. Phys. Lett.* **264**, 589 (1997).

³G. García, F. Blanco, and A. Willart, *Chem. Phys. Lett.* **335**, 227 (2001).

⁴S. Agostinelli *et al.*, *Nucl. Instrum. Methods Phys. Res. A* **506**, 250 (2003).

⁵F. Blanco and G. García, *Phys. Rev. A* **67**, 022701 (2003).

⁶F. Blanco and G. García, *Phys. Lett. A* **255**, 147 (1999).

⁷F. Blanco and G. García, *Phys. Lett. A* **295**, 178 (2002).

⁸N. F. Mott and H. S. W. Massey, *The Theory of Atomic Collisions* (Clarendon, Oxford, 1971).

⁹R. D. Cowan, *The Theory of Atomic Structure and Spectra* (University of California Press, London, 1981).

¹⁰M. E. Riley and D. G. Truhlar, *J. Chem. Phys.* **63**, 2182 (1975).

¹¹X. Z. Zhang, J. F. Sun, and Y. F. Liu, *J. Phys. B* **25**, 1893 (1992).

¹²R. D. DuBois and M. E. Rudd, *J. Phys. B* **9**, 2657 (1976).

¹³R. H. Jansen, F. J. de Heer, H. J. Luyken, B. van Wingerden, and H. J. Blaauw, *J. Phys. B* **9**, 185 (1976).

¹⁴J. P. Bromberg, *J. Chem. Phys.* **60**, 171 (1974).

¹⁵I. Iga, L. Mu-Tao, J. C. Nogueira, and R. S. Barbieri, *J. Phys. B* **20**, 1095 (1987).

¹⁶G. García and F. Manero, *Phys. Rev. A* **53**, 250 (1996).

¹⁷G. García, J. L. de Pablos, F. Blanco, and A. Willart, *J. Phys. B* **35**, 4657 (2002).

¹⁸F. Manero, F. Blanco, and G. García, *Phys. Rev. A* **66**, 032713 (2002).